Redox Biology 15 (2018) 266–276

Contents lists available at ScienceDirect

Redox Biology

journal homepage: www.elsevier.com/locate/redox

Research Paper

TiO_2 nanoparticles cause mitochondrial dysfunction, activate inflammatory responses, and attenuate phagocytosis in macrophages: A proteomic and metabolomic insight

Qun Chen[a,b,c,1], Ningning Wang[a,b,1], Mingjiang Zhu[a], Jianhong Lu[a,b], Huiqin Zhong[a,b], Xinli Xue[a,b], Shuoyuan Guo[a,b,c,d], Min Li[a,b], Xinben Wei[a,b], Yongzhen Tao[a], Huiyong Yin[a,b,c,d,*]

[a] Key Laboratory of Food Safety Research, Institute for Nutritional Sciences (INS), Shanghai Institutes for Biological Sciences (SIBS), Chinese Academy of Sciences (CAS), Shanghai, China
[b] University of the Chinese Academy of Sciences, CAS, Beijing, China
[c] Key Laboratory of Food Safety Risk Assessment, Ministry of Health, Beijing, China
[d] School of Life Science and Technology, ShanghaiTech University, Shanghai, China

ARTICLE INFO

Keywords:
TiO_2 nanoparticles
Macrophages
Mitochondrial dysfunction
Inflammation
Proteomics
Metabolomics

ABSTRACT

Titanium dioxide nanoparticles (TiO_2 NPs) are widely used in food and cosmetics but the health impact of human exposure remains poorly defined. Emerging evidence suggests that TiO_2 NPs may elicit immune responses by acting on macrophages. Our proteomic study showed that treatment of macrophages with TiO_2 NPs led to significant re-organization of cell membrane and activation of inflammation. These observations were further corroborated with transmission electron microscopy (TEM) experiments, which demonstrated that TiO_2 NPs were trapped inside of multi-vesicular bodies (MVB) through endocytotic pathways. TiO_2 NP caused significant mitochondrial dysfunction by increasing levels of mitochondrial reactive oxygen species (ROS), decreasing ATP generation, and decreasing metabolic flux in tricarboxylic acid (TCA) cycle from ^{13}C-labelled glutamine using GC-MS-based metabolic flux analysis. Further lipidomic analysis showed that TiO_2 NPs significantly decreased levels of cardiolipins, an important class of mitochondrial phospholipids for maintaining proper function of electron transport chains. Furthermore, TiO_2 NP exposure activates inflammatory responses by increasing mRNA levels of TNF-α, iNOS, and COX-2. Consistently, our targeted metabolomic analysis showed significantly increased production of COX-2 metabolites including PGD_2, PGE_2, and 15d-PGJ_2. In addition, TiO_2 NP also caused significant attenuation of phagocytotic function of macrophages. In summary, our studies utilizing multiple powerful omic techniques suggest that human exposure of TiO_2 NPs may have profound impact on macrophage function through activating inflammatory responses and causing mitochondrial dysfunction without physical presence in mitochondria.

1. Introduction

Engineered Nanoparticles have been widely used in food, cosmetics, and medicine due to their unique physical and chemical properties [1]. In particular, titanium dioxide (TiO_2) nanoparticles (NPs) are added to cosmetics, chewing gum, beverage, sauce and many other products. There are increasing concerns regarding the health effects of human exposure of these TiO_2 NPs, which have not been well defined [2–4]. In 2006, the International Agency for Research on Cancer (IARC) classified pigment-grade TiO_2 as suspected carcinogen (class 2B) [5]. As the first line of defence, macrophages try to clear these TiO_2 NPs through phagocytosis and protect the body from potential harm. However, it remains poorly define how TiO_2 NPs affect the immune functions and metabolism of macrophages upon exposure [6]. Liu et al. reported decreased chemotactic ability, MHC-class II expression on the cell surface and increased secretion of nitric oxide (NO) and tumour necrosis factor-alpha (TNF-α) in rat pulmonary macrophages after intra-tracheal instillation of TiO_2 NPs [7]. Exposure of TiO_2 NPs also activated inflammatory responses through upregulation of inflammatory cytokines in mouse bronchial alveolar lavage (BAL) fluid [8]. Furthermore, gastric ingestion or oral exposure of TiO_2 NPs caused similar immune responses in other animal experiments. Sang et al. found that serious

* Correspondence to: Institute for Nutritional Sciences, Shanghai Institutes for Biological Sciences, Chinese Academy of Sciences, Room A1826, New Life Science Building, 320 Yueyang Road, Shanghai 200031, China.
E-mail address: hyyin@sibs.ac.cn (H. Yin).
[1] These authors contribute equally to this work.

https://doi.org/10.1016/j.redox.2017.12.011
Received 30 August 2017; Received in revised form 15 December 2017; Accepted 21 December 2017
Available online 28 December 2017

spleen injury, increased level of nucleic factor-kappa B, TNF-α and interleukin secretion and decreased immunoglobulin in mice for long time intra-gastric exposure to TiO_2 NPs [9]. It still poorly understood how TiO_2 NP exposure affects immune responses. Limited studies suggested that TiO_2 NP exposure led to activated immune responses and elevation of ROS production and upregulation of pro-inflammatory factors, such as IL-1β, TNF-α, IFN-γ and IL-10 [10]. The macrophages function appeared to be affected, such as decreased phagocytic ability and chemotactic ability in exposed primary PAMs [11,12]. Furthermore, it remains controversial for the cellular locations of the TiO_2 NPs once they enter the immune cells even though there are some data suggesting that mitochondrial functions are significantly affected [13–15]. Moreover, TiO_2 beads are routinely used in enrichment of phosphorylated peptides and proteins in proteomic studies due to its strong binding with phosphate groups [16,17]. Thus we hypothesized that exposure of TiO_2 NPs in macrophage might have profound impact on the membrane phospholipids and phosphorylated proteins, which represents a unique property of TiO_2 NPs different from other metal oxide NPs.

In this study, we found that treatment of macrophage cell line (RAW) or primary mouse bone marrow-derived macrophages (BMDM) with TiO_2 NPs had marginal effects on cell viability but caused mitochondrial dysfunction and upregulated inflammation. Proteomic analysis of the entire proteome and phosphorylated proteome revealed massive membrane reorganization and activation of inflammation. These results were further supported by targeted metabolomic analysis of inflammatory pathways including metabolites from cyclo-oxygenases (COX) pathway, lipidomic analysis of mitochondrial phospholipids cardiolipin and metabolic flux from ^{13}C-labelled glutamine. All these omic data strongly suggest that mitochondria are the primary cellular targets for TiO_2 NPs in macrophages. Surprisingly, however, Transmission Electron Microscopy (TEM) experiments demonstrated that TiO_2 NPs were not present in mitochondria but were trapped inside of multi-vesicular bodies (MVB), suggesting an indirect effect of TiO_2 on mitochondrial function of macrophages. Furthermore, we performed functional studies to investigate the consequences of TiO_2 NP exposure and found that TiO_2 NPs caused significant attenuation of phagocytic function of macrophages. In summary, our data shed new light on potential impact of long term human exposure of TiO_2 NPs.

2. Material and methods

2.1. TiO_2 NPs and characterization

TiO_2 NPs were purchased from Beijing DK Nano Technology Co., Ltd. (Beijing, China) and were used in a previous publication [18]. The average NPs size was 10 nm and 99.9% pure Anatase. There was no LPS contamination as determined by the same method previously used. Roswell Park Memorial Institute (RPMI, Hyclone) 1640 complete medium and Dulbecco's modified Eagle's medium (DMEM, Gibco) complete medium were used as suspending agents. TiO_2 NPs powder was dispersed into the suspending solutions and then were treated by ultrasonic agitation for 30 min for better diffusion. We used 1 mg/ml TiO_2 NPs as a stock solution, and diluted it for work solution. TiO_2 NPs size measurements were performed using dynamic light scattering (DLS) instrument (Malvern Zetasizer, Nano-ZS90). A stock solution of 1 mg/ml was immediately diluted to 10 μg/ml and 100 μg/ml and measure the size distribution.

2.2. Transmission electron microscopy (TEM)

Cells were harvested after 24 h exposure and fixed by 2.5% paraformaldehyde and 2.5% glutaraldehyde and stained by osmium tetroxide, then were scanned by transmission electron microscopy (TEM, FEI Tecnau G2 spirit).

2.3. Cell culture

RAW 264.7 cell line was purchased from the Cell Bank of Chinese Academy of Sciences (Shanghai, China). Cells were cultured in DMEM supplemented with 10% fetal bovine serum (FBS, Gibco) and 1% penicillin-streptomycin (Gibco), incubated in an atmosphere of 95% air and 5% CO_2 constant temperature of 37 °C. RAW cells were seeded 8×10^5 cells /well and BMDM were seeded 1×10^6 cells/well in 6-well plates. All experiments were performed at least triplicates.

2.4. Isolation and culture of mouse Bone marrow derived macrophages (BMDM)

BMDM was separated from bone and matured by L929 (cell line was purchased from ATCC® CCL-1TM) supernatant as protocol described in the literature [19]. We isolated bone from C57BL/6Jslac mice and cultured the matured BMDM with RPMI 1640 complete medium, incubated in an atmosphere of 95% air and 5% CO_2 constant temperature of 37 °C. The animal studies were approved by the review committee from the Institute for Nutritional Science (Shanghai Institutes for Biologic Sciences, Chinese Academy of Sciences) and performed in accordance with the institutional guidelines.

2.5. MTT assay

Cell viability was determined by the (3-(4, 5-dimethylthiazaol-2-yl)-2,5-diphenyltertrazoliun bromide) (MTT) assay. Cells were seeded in a 96-well plate, after 24 h the medium was replaced by medium containing 0–100 μg/ml for 24 h incubation and added 10 ul 5 mg/ml MTT for 4 h, then adding 200ul DMSO for dissolving crystals, after centrifugation the supernatant was placed in a new 96-well plate and measured by multilabel reader (PE Enspire, Beijing, China).

2.6. Proteomic analysis

BMDM cells were treated with 100 μg/ml TiO_2 NPs in triplicates. After 24 h the cells were washed with phosphate-buffered saline solution (PBS) three times. Proteins in cells were extracted with lysis buffer containing protease inhibitors. The phosphorylated proteins were enriched by TiO_2 beads. The proteomic analyses were performed in Shanghai Applied Protein Technology Co. Ltd. (Shanghai, China). Eight plex iTRAQ (isobaric tags for relative and absolute quantitation) was performed using high resolution Q Exactive mass spectormeter (Thermo Scientific, San Jose, CA) coupled with cation exchange (SCX) nano-liquid chromatography separation.

2.7. Gas Chromatography- Mass Spectrometry (GC-MS)

RAW264.7 cells were seeded at a density of approximately 2×10^6 cells per 10 cm dish. After adhering, the cell culture medium was changed for labelling medium with ^{13}C-glutamine containing different concentrations of TiO_2 NPs. The medium of ^{13}C-glutamine composed of low glucose DMEM (Gibco1, 1054-020) was supplemented with the unlabelled 1 g/L glucose (Sigma-Aldrich, G7528), 10% (v/v) FBS, the labelled 2 mM L-glutamine-$^{13}C5$ (Sigma-Aldrich, 605166), 1% (v/v) antibiotic/antimycotic solution (Omega). Following the 24 h labelling period, cells were rinsed with phosphate buffer sodium (PBS), detached with trypsin and subjected to centrifugation at 500 × *g* for 5 min. Cells were centrifuged at 500 × *g* for 3 min. Cell pellets were re-suspended in 0.6 ml cold (− 20 °C) 50% aqueous methanol containing 100 μM Norvaline as an internal standard, frozen on dry ice for 30 min, then thawed on ice for 10 min before centrifugation. The supernatant was then partitioned with 0.3 ml chloroform to reduce the fatty acid content. The methanol layer was dried by centrifugal evaporation and stored at − 80 °C before analysis. Metabolites were derivatized for GC/MS analysis as follows: First, 50 μL of 20 mg/ml O-Isobutyl

hydroxylamine Hydrochloride (TCI® , I0387) was added to the dried pellet and incubated for 20 min at 80 °C 0.50 μL N-tert-butyl-dimethylsilyl-N-methyl- trifluoroacetamide (Sigma-Aldrich, 394882) was added after cooling and samples were re-incubated for 60 min at 80 °C before centrifugation for 5 min at 14,000 rpm (4 °C). The supernatant was transferred to an autosampler vial for GC/MS analysis. A Shimadzu QP-2010 Ultra GC-MS was programmed with an injection temperature of 250 °C injection split ratio 1/10 (depending upon sample concentration) and injected with 1 μL of sample. The GC column used was a 60 m × 0.25 mm × 0.25 μm Rxi®-5 ms (RESTEK®, 1134437). GC/MS data were analysed to determine isotope labelling of metabolites, all these procedures refer to this paper [20].

2.8. Phagocytosis

Cells were treated with GFP - *E. Coli* for 1 h after exposure to TiO_2 NPs for 24 h. After washed with PBS 5 times, cells were collected and detected GFP fluorescence intensity by flow cytometry (FACS Calibur) [21].

2.9. Prostaglandin analysis

Eicosanoid analysis by a targeted metabolomic approach was performed following a previously published protocol [22]. Cell medium was collected after 24 h exposure to TiO_2 nanoparticles in RAW and BMDM. Then we used 1 ml medium to abstract the prostaglandin by Hexane/MTBE solvents. Ultra-Performance Liquid Chromatography (UPLC) system (Shimadzu, Nexera® 20 A) was used. Reversed-phase separation was performed on a Phenomenex Kinetex column (100 × 2.1 mm; 2.6 μm; Phenomenex). The mobile phase consisted of (A) acetonitrile/water/acetic acid (60/40/0.02, v/v) and (B) acetonitrile/isopropyl alcohol (50/50, v/v); A 10 μL aliquot of each sample was injected onto the column. All samples were kept at 4 °C throughout the analysis. Mass spectrometry was performed on an ABI/ Sciex 5500 QTRAP hybrid of triple quadrupole and linear ion trap mass spectrometer. Eicosanoids were detected in negative electrospray ion mode. Curtain gas (CUR), nebulizer gas (GS1), and turbo-gas (GS2) were set at 10 psi, 30 psi, and 30 psi, respectively. The electrospray voltage was − 4.5 kV, and the turbo ion spray source temperature was 500 °C. Eicosanoids were analysed using scheduled multiple reaction monitoring (MRM). Nitrogen was employed as the collision gas. Data acquisitions and analysis were performed using Analyst 1.6.2 software (AB SCIEX).

2.10. Real Time-PCR

Cells were rinsed with PBS and total RNA was extracted from the cells using Trizol reagent (Takara) according to its manufacture's protocol. RNA concentration was measured by ND-1000 spectrophotometer (Thermo Scientific, USA) and 800 ng RNA was normalized each sample to react with reverse transcriptase, then the resulting cDNA was mixed with primers for target genes and Syber Green master mix to assess the levels of mRNA expression by RT-PCR using a 7900 Real-Time PCR system (Applied Biosystems). The qPCR reaction was performed with an initial denaturation step of 10 min at 95 °C, followed by 25 s at 95 °C, 60 s at 60 °C and 30 s at 72 °C for 40 cycles. The mRNA levels of each genes were normalized relative to the levels of L32.

2.11. Quantification of Cardiolipins by a targeted lipidomics based on liquid chromatography – mass spectrometry (LC–MS/MS)

The cells exposed to TiO_2 NPs for 24 h were adding sodium chloride (NaCl) solution and homogenized. The lipids were extracted by the chloroform and methanol (2:1) and the organic phase was evaporated by gentle flow of N_2, re-suspended in mobile phase A and stored at − 80 °C until analysis. The cardiolipin analysis by LC-MS was performed according to previous published studies. [23,24].

2.12. Reactive oxygen species detection

MitoSOX™ Red mitochondrial superoxide indicator (life technologies, M36008) was used for detecting the mitochondrial ROS. Cells were seeded in the plate with slides and treated by TiO_2 NPs for 24 h, then were washed with PBS, adding the 5 μM reagent solution, to cover cells adhering to coverslip. Incubated cells for 10 min at 37 °C, protected from light according to the manufacture protocol. The ROS was detected by confocal (FV1000, Olympus). All measurements were performed to exclude the interference from TiO_2 NP.

ROS were also measured by dihydroethidium and high performance liquid chromatography assay as described previously [25,26].

2.13. Statistical analysis

Data are presented as mean + SEM. Differences between two groups were analysed by 2-tailed, unpaired Student *t*-tests using GraphPad Prism 5.0 (GraphPad Software). Each group has three replicates, P-values < 0.05 were considered statistically significant.

3. Results

3.1. Size distribution in cell media and cytotoxicity of TiO_2 NPs

We used Dynamic Light Scattering (DLS) to measure the size distributions of TiO_2 NPs in the cell media RPMI 1640 and DMEM complete medium, both of which were used in the cell culture studies. As shown in the Supplemental Figure 1S, 10 and 100 μg/ml TiO_2 NPs mainly distributed in 100–300 nm in RPMI 1640 complete medium and similar observations were made for DMEM complete medium.

To study the cytotoxicity of TiO_2 NPs for macrophages, we exposed different concentrations of TiO_2 NPs to RAW 264.7 cell lines and primary BMDM for 24 h and performed cell viability assay. As shown in Fig. 2S, TiO_2 NPs did not significantly affect cell viability until 100 μg/ml in RAW (Fig. S2A) and 10 μg/ml in BMDM (Fig. S2B) respectively, suggesting that TiO_2 NPs have minimal cytotoxicity. To further verify cytotoxicity, we used trypan blue staining and the data were shown in Fig. S2C.

3.2. Proteomic and phosphoproteomic analysis revealed that TiO_2 NPs caused significant membrane alterations and inflammatory responses

To investigate the global responses of macrophages to TiO_2 NPs, we performed proteomic analysis on primary macrophages treated with 100 μg/ml TiO_2 NPs. As shown in Fig. 1, we found that distinct patterns of entire proteome and phosphoproteome were affected by TiO_2 NP treatment. Around 1000 proteins were differentially expressed for entire proteome and phosphorylated proteome, among them 40% at the proteome level and 56% for phosphorylated proteins (Supplemental Fig. S3). These observations were consistent with our hypothesis in which TiO_2 NPs have more profound impact on the phosphorylated proteins due to the strong interaction with phosphates. At a proteome level, the biological processes (BP) that were significantly affected included cellular component assembly, localization of cell, homeostasis, cell growth, and transmembrane receptor proteins in tyrosine kinase signalling pathways (Fig. 1B). On the other hand, the significantly altered phosphorylated proteins were those involved in regulation of adaptive immune response, receptor mediated phagocytosis, and anion transmembrane transport (Fig. 1D, Table 1S and 2S). We performed further analysis of these biological processes into cellular component (CC) and molecular functions (MF). At the proteome level, these significantly altered cellular components were cytoskeleton, extracellular region, intermediate filament cytoskeleton, mitochondrial outer membrane translocase complex. Similar changes were observed at phosphoproteome level: regulation of cell morphogenesis, tubulin complex, transcriptional repressor complex, endoplasmic reticulum (ER)

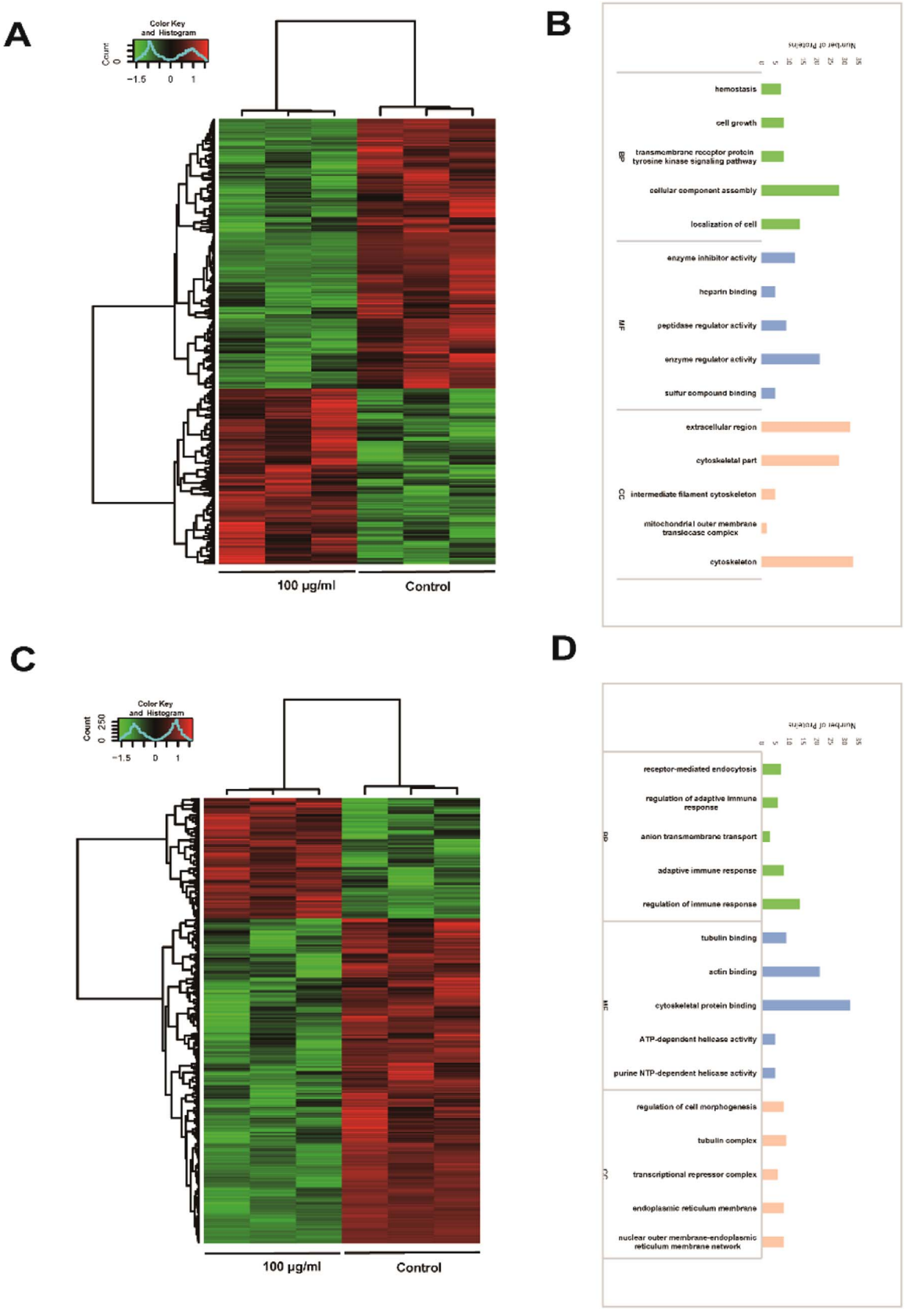

Fig. 1. Proteomic analysis of TiO_2 NP exposure in BMDM. (A) The heat map of differential total protein expression profiles. The color scale (left) illustrates the relative expression level across all sample. Green indicates proteins that were significantly downregulated while red indicates significantly upregulated proteins. (B) The functional assignments in total protein profiles with biological processes (green), molecular functions (blue), and cellular components (pink) are shown from the number of proteins. The specific proteins are listed in Supplementary Table S1. (C) The heat map of differential phosphorylated protein expression profiles in BMDMs. (D) The functional assignments in phosphorylated protein profiles with biological processes (green), molecular functions (blue), and cellular components (pink) are shown from the number of proteins. The specific proteins are listed in Supplementary Table S2. The experiments were performed in triplicates.

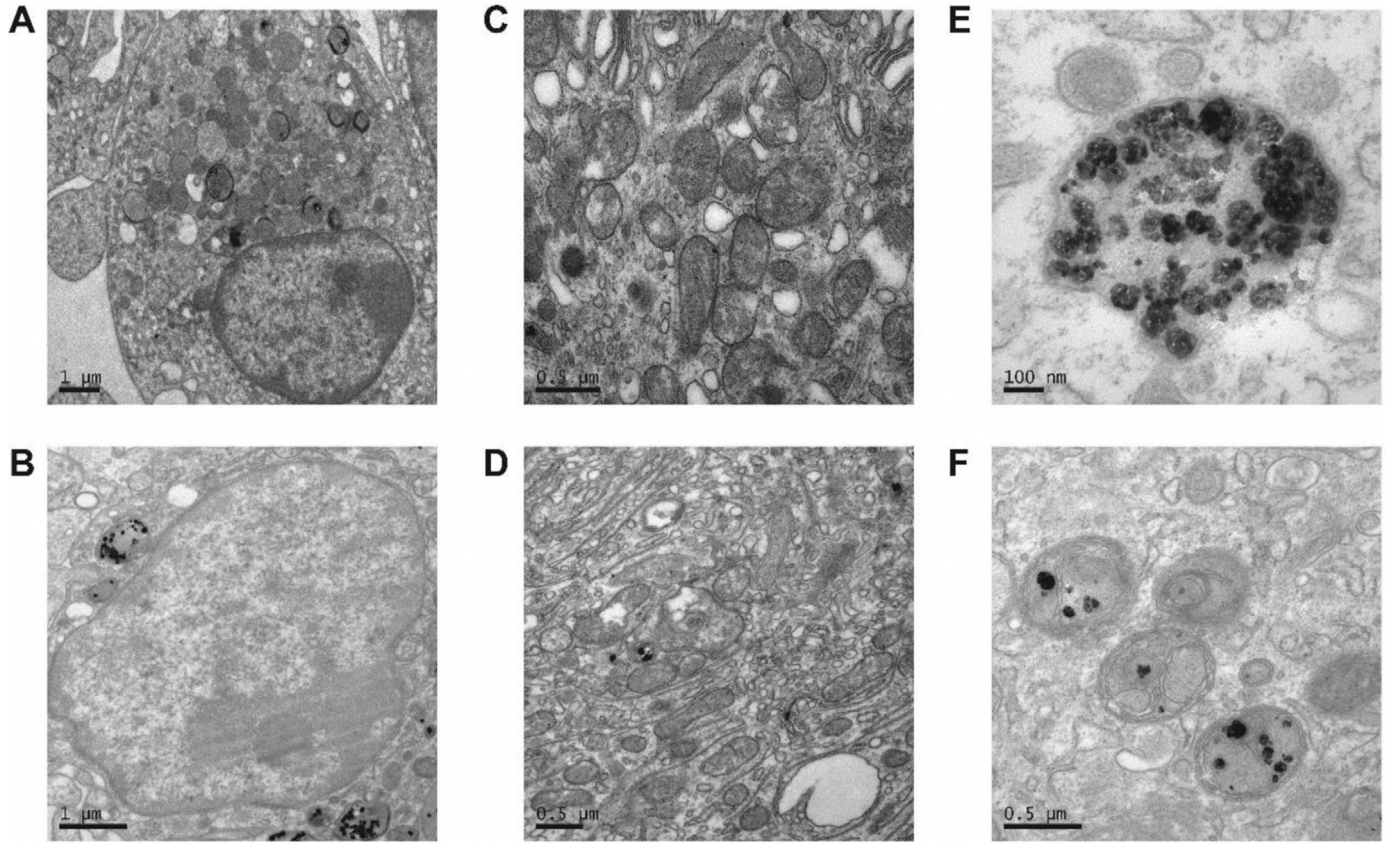

Fig. 2. TEM analysis of BMDM with TiO_2 NPs: (A) Control samples without NPs; (B) BMDM incubated with NPs; (C) Mitochondria in control cells; (D) cells treated with NPs. NPs were trapped in MVB in BMDM cells (E) and (F).

membrane, and the networks between ER and nuclear outer membrane. These phosphorylated proteins were critical for molecular functions, such as tubulin and actin binding, cytoskeleton protein binding, ATP-dependent and purine NTP-dependent helicase activities. Taken these data together, TiO_2 NP exposure caused massive membrane re-organization, both at cytoplasm and organelle levels, and immune responses. Furthermore, TiO_2 NPs had a profound impact on the phosphoproteome, which most likely represents a unique feature for TiO_2 due to its strong interactions with phosphate groups in proteins and phospholipids.

3.3. TiO_2 NPs were exclusively trapped in multi-vesicular bodies (MVB) in BMDM as analysed by TEM

From proteomic analysis, cellular membranes were significantly affected by TiO_2 NPs. We next used TEM to investigate the structural changes of BMDM cells after TiO_2 NP treatment. As shown in Fig. 2, TiO_2 NPs were indeed endocytosed into macrophages. Interestingly, however, NPs did not enter into nucleus nor mitochondria (Fig. 2D). Instead, upon 24-h exposure, TiO_2 NPs were trapped inside of multi-vesicular bodies (MVB), morphologically similar to endocytic vesicles or lamellar bodies. These results were consistent with the proteomic studies in which proteins involved in endocytotic pathways were among the most significantly affected. Our further analysis of these protein profiles found that the proteins of Clathrin-dependent phagocytosis had significantly changed (data not shown), suggesting that TiO_2 NPs entered the macrophages via Clathrin-dependent pathways. Consistently, proteins involved in the early endosome, late endosome, and multi-vesicular bodies were also changed significantly.

3.4. TiO_2 NPs decreased the ATP production and altered the metabolism of TCA cycle

Even though our TEM studies did not find TiO_2 NPs in mitochondria, our proteomic studies revealed that mitochondrial membranes and function appeared to be affected, corroborating with accumulating evidence that nanoparticles target mitochondria after they entered the cells. As the power house of a cell, ATP is predominantly produced in mitochondria and the level of ATP is a sensitive measure for mitochondrial function. As shown in Fig. 3, the levels of ATP were dose-dependent attenuated in both RAW and BMDM after incubation of TiO_2 NPs.

ATP production and oxidative phosphorylation are carried out in the tricarboxylic acid (TCA) cycle in mitochondria. To provide further evidence for the mitochondrial dysfunction upon TiO_2 NP exposure, we performed metabolic flux analysis using GC-MS technique to study the alteration of metabolism in TCA cycle. Universally labelled ^{13}C-glutamine was employed as a tracer to track the metabolites in TCA cycle. As shown in Fig. 3C (^{13}C atoms are depicted as filled blue cycles), the U-^{13}C glutamine transformed into glutamic acid, which was metabolized into α-ketoglutarate (α-KG) and entered the TCA. TCA metabolic efflux was assessed by analysing the isotopomer distribution of indicated metabolites in cells derived from [U-^{13}C13] glutamine. As shown in Fig. 3D, we observed a dose-dependent decrease of metabolic flux in most TCA metabolites after 24 h exposure of TiO_2 NPs in RAW cell. Collectively, TiO_2 NP exposure to macrophages caused significant mitochondrial dysfunction resulting in down-regulation of metabolism in TCA cycle and ATP production.

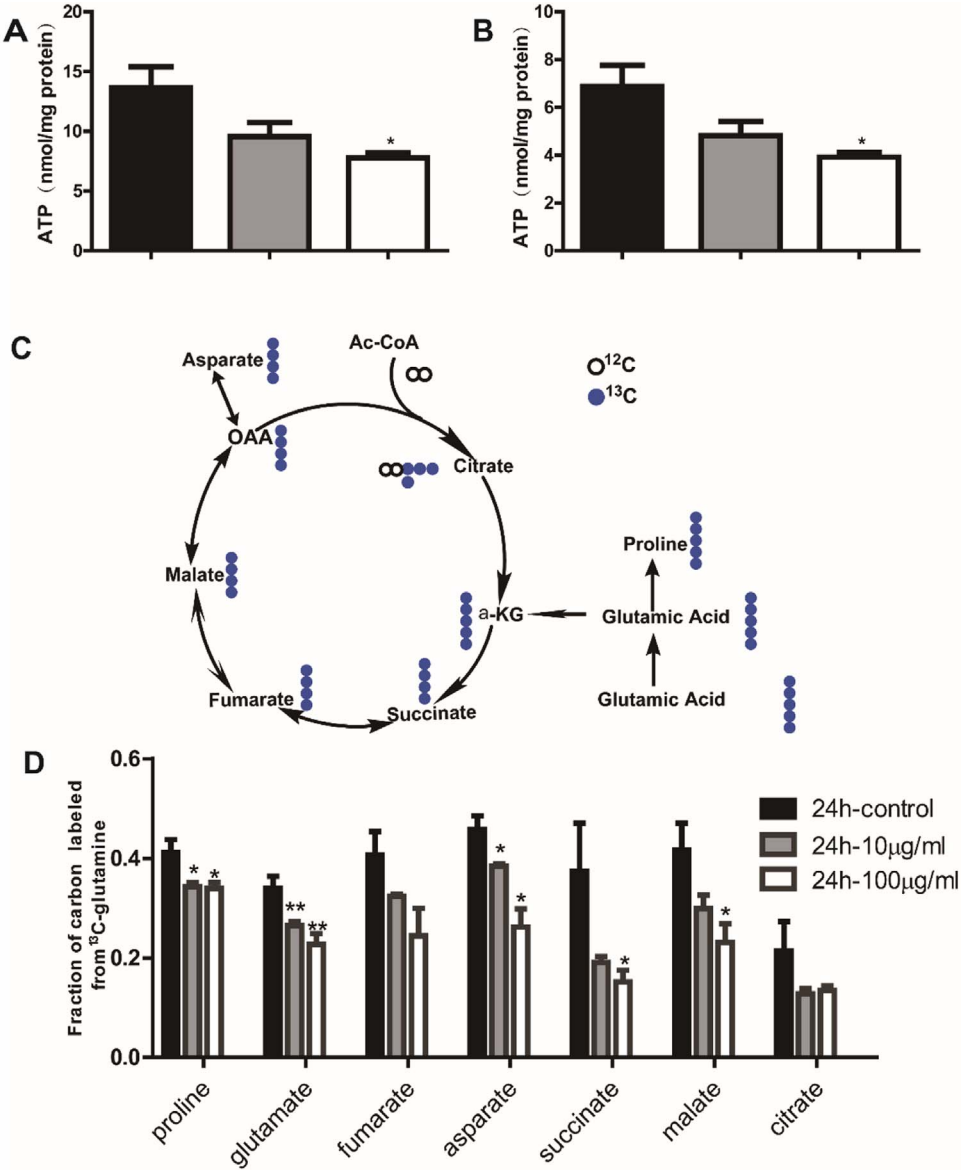

Fig. 3. TiO_2 NPs exposure attenuated the production of ATP and mitochondrial metabolism of TCA cycle. Levels of ATP in RAW cell lines (A) and BMDM cells (B); Metabolic flux analysis of TCA using the ^{13}C () labelled glutamine U-^{13}C glutamine and GC-MS analysis (C); metabolites in TCA cycle after incubation with different concentrations of TiO_2 NPs (D).

3.5. TiO_2 NP exposure causes deceased levels of mitochondrial cardiolipin and enhanced ROS production in macrophages

Cardiolipin (CL) is a unique class of phospholipids primarily present in mitochondrial inner membrane and critical for maintaining proper function of multiple protein complexes in the electron transport chain (ETC) [27,28]. After we observed the down-regulation of ATP and TCA cycle metabolism, we set out to study the CL profile using a state-of-the-art lipidomic approach [29–31]. As shown in Fig. 4, most CL species were significantly down-regulated, suggesting a dysfunctional ETC upon TiO_2 NP exposure (Supplemental Table 3). Furthermore, mitochondria are the major cellular sites for ROS production and maintaining proper ROS level is critical for mitochondrial function. As shown in Fig. 5, we found that incubation with TiO_2 NPs significantly increased the ROS production in mitochondria in BMDM. To further verify the ROS production, we also used HPLC method to measure the ROS levels. As shown in Fig. 5E, ROS increased after TiO_2 NPs stimulation in BMDM.

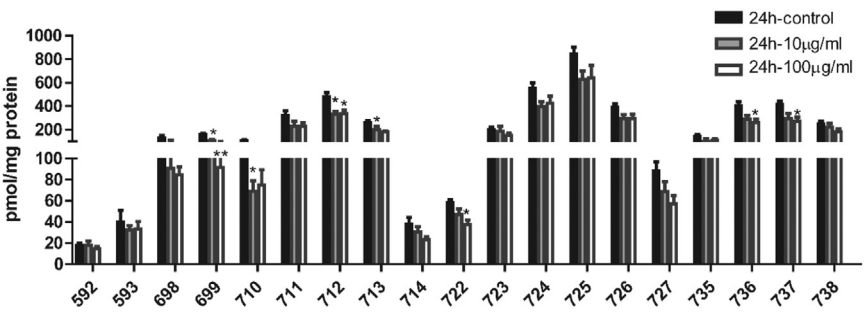

Fig. 4. Profiles of mitochondrial cardiolipin after 24-h exposure with TiO_2 NPs analysed by a MS-based lipidomics.

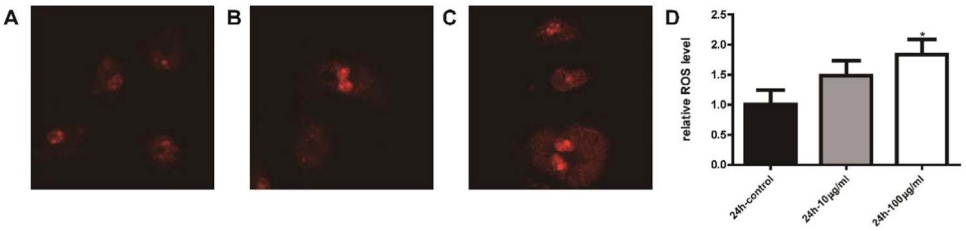

Fig. 5. ROS production in macrophages after exposure of TiO_2 NPs.

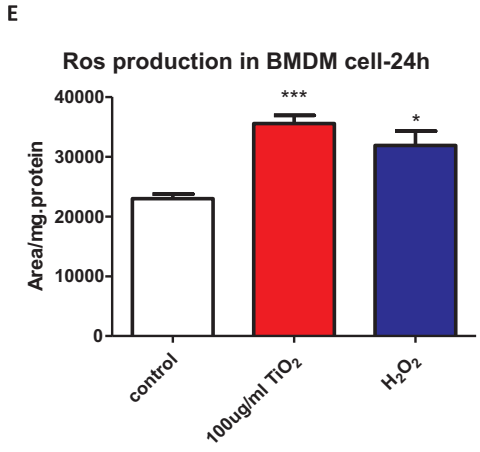

Our previous studies found that oxidation of CL and generation of reactive lipid mediators from CL oxidation played an important role in modulation of mitochondrial function and apoptosis [24,27,32]. However, we did not observe elevation of oxidized CL upon TiO_2 NPs exposure (data not shown), suggesting a modest degree of mitochondrial dysfunction that is well below the threshold of inducing apoptotic cell death. Collectively, TiO_2 NPs exposure causes down-regulation of CL and elevated production of ROS in macrophages, suggesting that TiO_2 NP exposure causes mitochondrial dysfunction.

3.6. TiO_2 NPs exposure activates inflammatory responses

As one of the most important classes of immune cells in human body, macrophages respond to inflammatory stimuli by up-regulation of inflammatory genes such as cyclooxygenases (COX), TNFα, and iNOS. Our proteomic studies also suggested that TiO_2 NPs significantly activated inflammatory response. We observed dose-dependent increase of TNFα and iNOS upon treatment of TiO_2 NPs in RAW and BMDM cells (Fig. 6). Furthermore, COX-2 pathway is critical for inflammatory responses in macrophages. As shown in Fig. 7A, upon inflammatory stimulation, arachidonic acid (AA) in cell membrane can be released by PLA_2 and COX-2 enzyme acts on the free AA to generate PGH_2. The latter is turned into PGD_2, PGE_2, and $PGF_{2\alpha}$ by their respective synthases; 15d-PGJ_2 is formed from dehydration of PGD_2 through non-enzymatic process. These prostaglandins elicit inflammatory responses though interactions with their respective G-protein coupled receptors on the cell membrane in an autocrine or paracrine fashion [33]. We first found that TiO_2 NPs activated COX-2 pathway in macrophages (Fig. 7A) at the mRNA levels of COX-2 both in RAW cells and BMDM (Fig. 7B and D). Then we used a targeted metabolomics approach to accurately quantify all the metabolites derived from arachidonic acid and detected a significant increase of PGD_2, PGE_2, and 15d-PGJ_2 after 24-h exposure to a concentration of 100 μg/ml in RAW (Fig. 7C) and BMDM (Fig. 7E) respectively. Collectively, exposure of TiO_2 NPs in macrophages elicits inflammatory responses through up-regulation of COX-2 pathways and inflammatory genes including TNFα and iNOS.

3.7. TiO_2 NPs attenuates the phagocytic capability of macrophages

Besides the inflammatory responses, macrophages phagocytose invading foreign objects as the first line of defence in human body. To examine the effects of TiO_2 NP exposure on the phagocytic capability of macrophages, we pre-treated macrophages with different concentration of TiO_2 NP for 24 h before loaded the cells with green fluorescent protein (GFP) labelled E. coli and detected the fluorescence intensity by FACS. As shown in Fig. 8, the phagocytic function of macrophages was significantly attenuated upon TiO_2 NP exposure, suggesting a potential detrimental effect of immune responses upon human exposure of TiO_2 NPs.

4. Discussion

TiO_2 NPs are widely used in cosmetic, food and other dietary products due to their attractive chemical and physical properties. However, the health concerns regarding TiO_2 NP exposure remains to be resolved. Using macrophages as a model system, we observed a significant effects on human immune responses upon TiO_2 NP exposure characterized by mitochondrial dysfunction, elevated inflammatory responses, and attenuated phagocytic capability of macrophages (Fig. 9). Our studies highlighted a potential detrimental effect of TiO_2 NPs on human immune responses. Surprisingly, however, our studies by TEM revealed that TiO_2 NPs were trapped inside of MVBs in macrophages.

First of all, proteomics is a powerful tool to systematically investigate the proteome changes and this technique has been extensively employed to study the effects of nanoparticles. A comparative proteomic study of pulmonary TiO_2 nanoparticle exposure in rats identified three major biological pathways that were affected: reactive oxygen species, blood coagulation and liver damage [34]. Another proteomic study investigated the early response of unicellular eukaryotic protozoan *Tetrahymena thermophila* exposed to TiO_2-NPs and found alterations in metabolic pathways including lipid and fatty acid metabolism, purine metabolism, energetic metabolism, salt stress and protein degradation [35]. A later study using proteomics and metabolomics demonstrated that TiO_2 NPs resulted in upregulation of proteins and metabolites related to energy and growth metabolism [36]. Our

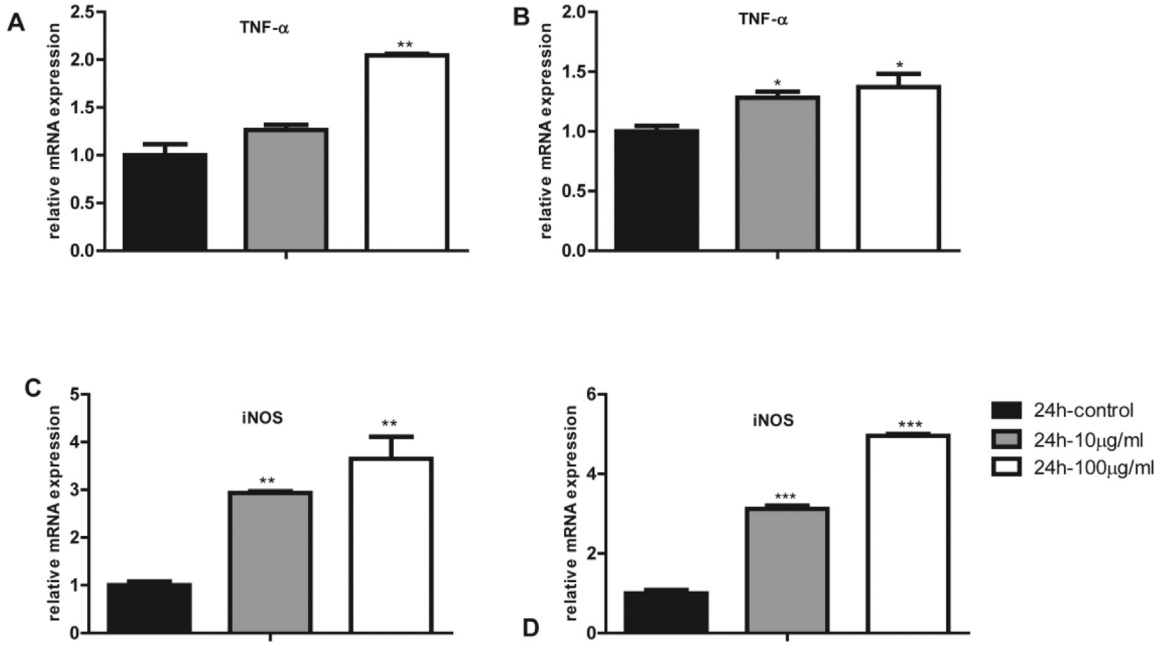

Fig. 6. The mRNA levels of inflammatory mediators in macrophages after TiO_2 NP exposure: TNF-αin RAW cell (A) and BMDM cell (B), iNOS in RAW cell (C) and BMDM cell (D).

proteomic studies identified, for the first time, that TiO_2 NP exposure had profound impact on the cellular membranes and adaptive immune responses (Fig. 1). The effects on cell membranes were consistent with a previous study demonstrating that an atypical macropinocytic-like mechanism mediated the entry of nanoparticles in HeLa and human mesenchymal stem cells [37]. We further observed a more significant alterations of phosphoproteome than the entire proteome, consistent with our hypothesis that TiO_2 NPs may preferentially act on phosphate groups in phosphorylated proteins and phospholipids. These effects may represent a unique property for TiO_2 NP, different from other metallic nanoparticles.

Secondly, we observed that the nanoparticles were exclusively trapped in MVBs. Even though a previous study suggested that trapping nanoparticles in MVB played an important role in cellular trafficking and storage of nanoparticles in HeLa and human mesenchymal stem cells [37], our study represented the first report that TiO_2 NPs were probably endocytosed and trapped in MVBs by a Clathrin-dependent pathway. It is conceivable that the cell membrane changes, including the formation of endosome and MVB, may lead to the functional alterations of macrophages.

Thirdly, we found that mitochondria were the primary targets for TiO_2 NPs: a decrease of ATP production, attenuated metabolic flux to TCA cycle, decreased cardiolipin profiles while a significant increase in mitochondrial ROS levels. Our studies were consistent with a previous report that TiO_2 NPs exposure decreased ATP in A549 cells [14,38,39]. In our study, we quantified the ATP levels after 24-h exposure of TiO_2 NPs to RAW 264.7 and BMDM and observed a dose-dependent decrease of ATP production (Fig. 3), an indication of mitochondrial dysfunction because ATP are primarily produced in mitochondria through oxidative phosphorylation in TCA cycle. Consistently, we used a targeted metabolomics approach to quantify the metabolic flux to TCA cycle using ^{13}C labelled glutamine as a tracer. Our metabolic flux analysis clearly demonstrated that a majority of the TCA metabolites were dose-dependently decreased upon TiO_2 exposure (Fig. 4D). A decreased mitochondrial function is further supported by our observation that TiO_2 NP exposure led to a significant decrease of CL, a unique class of mitochondrial phospholipids which are important in maintaining proper structure and function of multiple protein complexes including electron transport chain in mitochondria (Fig. 4). A significantly decrease in multiple molecular species of CL signalled a dysfunctional electron transport chain, which is consistent with decreased ATP production and elevated levels of mitochondrial ROS (Fig. 5). Interestingly, however, we did not observe an increased level of oxidized CL upon TiO_2 NP exposure even though our previous studies demonstrated that elevated ROS production in mitochondria may lead to apoptotic cell death resulted from CL oxidation and generation of reactive lipid mediators, such as 4-hydroxynonenal (4-HNE) [24,27,40]. Thus these data suggested that the mitochondrial dysfunction caused by TiO_2 NP exposure were rather modest and not enough to cause apoptosis in macrophages [41].

Lastly, we observed a significant impact of TiO_2 NP exposure on the immune responses and attenuation of phagocytic capability of macrophages, suggesting a health concern upon long term exposure. Our proteomic analysis showed that the immune response was significantly affected with the upregulation of the Complement C3, Complement component 4B and Thrombospondin-1. Our studies are consistent with previous reports that nanoparticles may elicit inflammatory response. A previous report suggested that ROS could trigger pro-inflammatory responses via activating redox sensitive MAPK and NF-κB signalling pathway [42]. Sang et al. found that serious spleen injury, increased level of nucleic factor-kappa B, TNF-α and interleukin secretion and decreased immunoglobulin and lymphocyte subsets of mice for long time intra-gastric exposure to TiO_2 NPs [9]. Furthermore, TiO_2 NPs activated immune cells, caused ROS production and upregulation of secreted pro-inflammatory factors, such as IL-1β, TNF-α, IFN-γ and IL-10 [43]. Macrophage functions were affected as indicated by decreased phagocytic ability and chemotactic ability in primary pulmonary alveolar macrophages (PAMs) [11]. COX-2 is an important rate limiting enzyme in the production of prostaglandins from arachidonic acid and these lipid mediators are involved in inflammation. Using a targeted metabolic approach, we found that the downstream metabolites of COX-2, PGD_2, PGE_2, and 15d-PGJ_2, were increased significantly upon exposure to TiO_2 NPs. In addition, mRNA levels of TNF-α and iNOS were also increased. Our studies were consistent with a previous report that mitochondria played an important role in innate immunity in macrophages, causing NLRP3 inflammasome, and promoting the pro-inflammatory responses [44].

In summary, our studies using multiple powerful omic techniques identified that TiO_2 NP exposure caused massive membrane alterations and elicited inflammatory responses. These observations were further

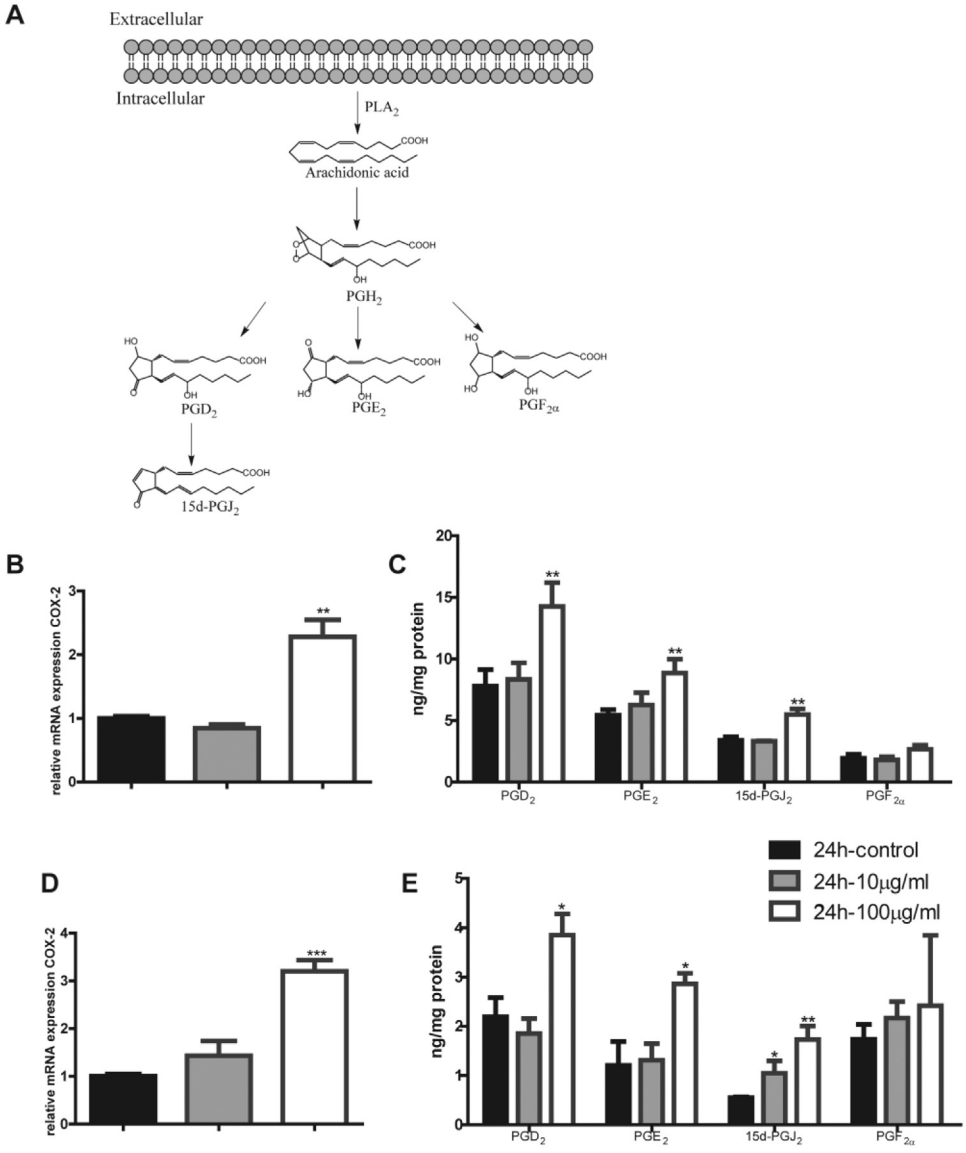

Fig. 7. TiO_2 NPs activate COX-2 pathways in macrophages. (A) Illustration of COX pathways and the related metabolites. (B) The mRNA level of COX-2 gene expression in RAW 264.7 cells. (C) The metabolites of COX pathways: PGD_2, PGE_2, 15d-PGJ_2, and $PGF_{2\alpha}$ in RAW 264.7 cells. (D) The mRNA level of COX-2 gene expression in BMDM. (E) The metabolites of COX pathways: PGD_2, PGE_2, 15d-PGJ_2, and $PGF_{2\alpha}$ BMDM.

solidified by TEM studies demonstrating that TiO_2 NPs were primarily trapped in MVB. Even though TiO_2 NPs were not physically present in mitochondria, mitochondrial functions are drastically affected, characterized by a significant decrease of ATP production and metabolic flux to TCA cycle, presumably through elevated ROS generation caused by a dysfunctional electron transport chain due to down-regulation of CL in mitochondria. Our subsequent functional studies pointed to an attenuated phagocytosis of macrophages. Collectively, our studies provided strong evidence that long term human exposure of TiO_2 NPs may elicit adverse effects on immunes responses and these health concerns of nanoparticle exposure warrant further investigation [45].

Acknowledgements

This work was financially supported by the National Key R&D Program of China administered by Chinese Ministry of Science and Technology (MOST) (2016YFD0400205, 2016YFC0903403), National Natural Science Foundation of China (31470831, 21402221, 31401015, 91439103, 91539127), and a grant from the Chinese Academy of Sciences (ZDBS-SSW-DQC-02). We would like to acknowledge the help on identification of MVB from Drs. Yoshikazu Uchida and Peter M Elias in the Department of Dermatology at University of California San Francisco.

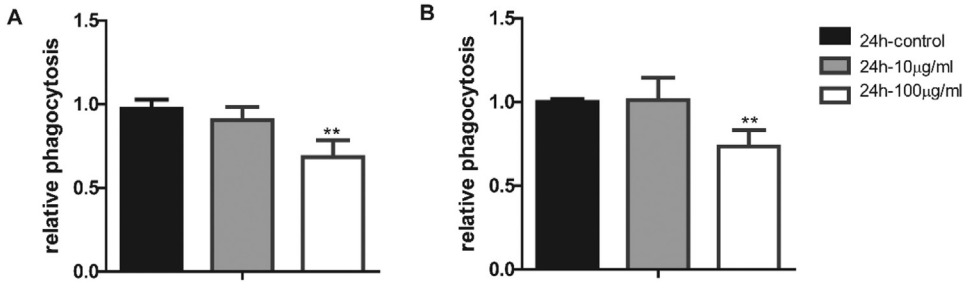

Fig. 8. TiO_2 NP exposure attenuates phagocytosis in RAW (A) and BMDM (B) cell.

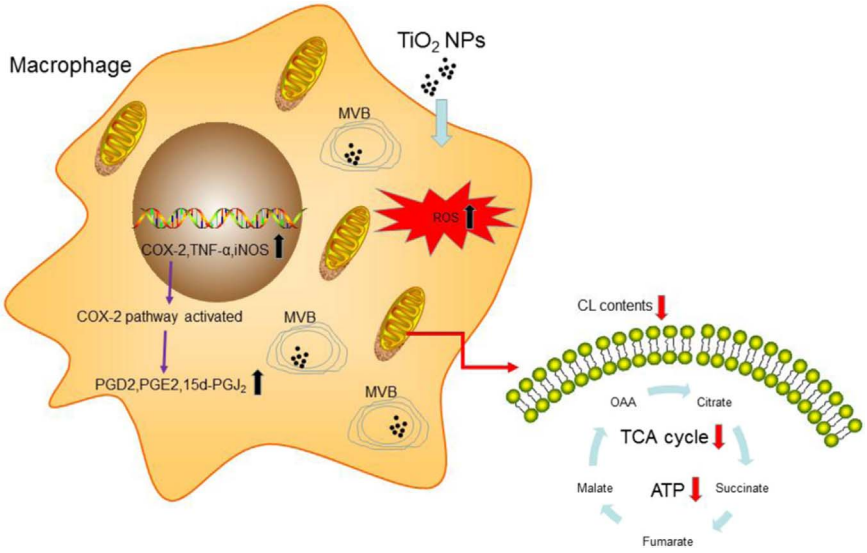

Fig. 9. Summary: impact of TiO_2 NPs on macrophage metabolism and functions.

Appendix A. Supporting information

Supplementary data associated with this article can be found in the online version at http://dx.doi.org/10.1016/j.redox.2017.12.011

References

[1] A. Martirosyan, Y.J. Schneider, Engineered nanomaterials in food: implications for food safety and consumer health, Int. J. Environ. Res. Public Health 11 (2014) 5720–5750.

[2] A. Weir, P. Westerhoff, L. Fabricius, K. Hristovski, N. von Goetz, Titanium dioxide nanoparticles in food and personal care products, Environ. Sci. Technol. 46 (2012) 2242–2250.

[3] B. Jovanovic, Critical review of public health regulations of titanium dioxide, a human food additive, Integr. Environ. Assess. Manag. (2014).

[4] Y. Yang, et al., Characterization of food-grade titanium dioxide: the presence of nanosized particles, Environ. Sci. Technol. 48 (2014) 6391–6400.

[5] Carbon Black, Titanium Dioxide, and Talc, IARC Monographs on the Evaluation of Carcinogenic Risks to Humans/World Health Organization, International Agency for Research on Cancer 93, 2010, 1-413.

[6] E. Frohlich, Value of phagocyte function screening for immunotoxicity of nanoparticles in vivo, Int. J. Nanomed. 10 (2015) 3761–3778.

[7] R. Liu, et al., Small-sized titanium dioxide nanoparticles mediate immune toxicity in rat pulmonary alveolar macrophages in vivo, J. Nanosci. Nanotechnol. 10 (2010) 5161–5169.

[8] V.H. Grassian, P., T. O'Shaughnessy, A. Adamcakova-Dodd, J.M. Pettibone, P.S. Thorne, Inhalation exposure study of titanium dioxide nanoparticles with a primary particle size of 2 to 5 nm, Environ. Health Perspect. 115 (2007) 397–402.

[9] X. Sang, Z. Zhang, F. Hong, The chronic spleen injury of mice following long-term exposure to titanium dioxide nanoparticles, J. Biomed. Mater. Res. Part A 100 (2012) 894–902.

[10] B.C. Schanen, W.L. Warren, W.T. Self, Exposure to titanium dioxide nanomaterials provokes inflammation of an in vitro human immune construct, ACS Nano 3 (2009) 2523–2532.

[11] R. Liu, X.Y. Zhang, The immune toxicity of titanium dioxide on primary pulmonary alveolar macrophages relies on their surface area and crystal structure, J. Nanosci. Nanotechnol. 10 (2010) 8491–8499.

[12] S. Kongseng, et al., Cytotoxic and inflammatory responses of TiO2 nanoparticles on human peripheral blood mononuclear cells, J. Appl. Toxicol.: JAT (2016).

[13] E. Huerta-Garcia, et al., Titanium dioxide nanoparticles induce strong oxidative stress and mitochondrial damage in glial cells, Free Radic. Biol. Med. 73 (2014) 84–94.

[14] V. Natarajan, S. Kidambi, Titanium dioxide nanoparticles trigger loss of function and perturbation of mitochondrial dynamics in primary hepatocytes, PLoS One 10 (2015) e0134541.

[15] Y. Tang, C. Jin, X. Zhong, Y. Yang, Mitochondrial injury induced by nanosized titanium dioxide in A549 cells and rats, Environ. Toxicol. Pharmacol. 36 (2013) 66–72.

[16] C.L. Nilsson, Advances in quantitative phosphoproteomics, Anal. Chem. 84 (2011) 735–746.

[17] A.M. Palumbo, et al., Tandem mass spectrometry strategies for phosphoproteome analysis, Mass Spectrom. Rev. 30 (2011) 600–625.

[18] C. Huang, et al., Titanium dioxide nanoparticles prime a specific activation state of macrophages, Nanotoxicology 11 (2017) 737–750.

[19] W. Ying, P.S. Cheruku, F.W. Bazer, S.H. Safe, B. Zhou, Investigation of macrophage polarization using bone marrow derived macrophages, J. Vis. Exp.: JoVE (2013).

[20] L. Ma, et al., Control of nutrient stress-induced metabolic reprogramming by PKCzeta in tumorigenesis, Cell 152 (2013) 599–611.

[21] L. Kong, et al., An essential role for RIG-I in toll-like receptor-stimulated phagocytosis, Cell host Microbe 6 (2009) 150–161.

[22] Y. Huang, et al., Mass spectrometry-based metabolomic profiling identifies alterations in salivary redox status and fatty acid metabolism in response to inflammation and oxidative stress in periodontal disease, Free Radic. Biol. Med. 70 (2014) 223–232.

[23] H. Yin, et al., Acetaminophen inhibits cytochrome c redox cycling induced lipid peroxidation, Biochem. Biophys. Res. Commun. 423 (2012) 224–228.

[24] H. Zhong, H. Yin, Formation of electrophilic oxidation products from mitochondrial cardiolipin in vitro and in vivo in the context of apoptosis and atherosclerosis, Redox Biol. 2 (2014) 878–883.

[25] X.N. Sun, et al., T-cell mineralocorticoid receptor controls blood pressure by regulating interferon-gamma, Circ. Res. 120 (2017) 1584–1597.

[26] S. Dikalov, K.K. Griendling, D.G. Harrison, Measurement of reactive oxygen species in cardiovascular studies, Hypertension 49 (2007) 717–727.

[27] H. Yin, M. Zhu, Free radical oxidation of cardiolipin: chemical mechanisms, detection and implication in apoptosis, mitochondrial dysfunction and human diseases, Free Radic. Res. 46 (2012) 959–974.

[28] M. Schlame, M.L. Greenberg, Biosynthesis, remodeling and turnover of mitochondrial cardiolipin, Biochim. Biophys. Acta (BBA) - Mol. Cell Biol. Lipids 1862 (2017) 3–7.

[29] H. Zhong, J. Lu, L. Xia, M. Zhu, H. Yin, Formation of electrophilic oxidation products from mitochondrial cardiolipin in vitro and in vivo in the context of apoptosis and atherosclerosis, Redox Biol. 2 (2014) 878–883.

[30] H. Zhong, et al., Mitochondrial control of apoptosis through modulation of cardiolipin oxidation in hepatocellular carcinoma: a novel link between oxidative stress and cancer, Free Radic. Biol. Med. 102 (2017) 67–76.

[31] H. Zhong, H. Yin, Role of lipid peroxidation derived 4-hydroxynonenal (4-HNE) in cancer: focusing on mitochondria, Redox Biol. 4 (2015) 193–199.

[32] W. Liu, N.A. Porter, C. Schneider, A.R. Brash, H. Yin, Formation of 4-hydroxynonenal from cardiolipin oxidation: intramolecular peroxyl radical addition and decomposition, Free Radic. Biol. Med. 50 (2011) 166–178.

[33] H. Yin, et al., Role of mitochondria in programmed cell death mediated by arachidonic acid-derived eicosanoids, Mitochondrion 13 (2013) 209–224.

[34] M.M. Maurer, et al., Comparative plasma proteomic studies of pulmonary TiO2 nanoparticle exposure in rats using liquid chromatography tandem mass spectrometry, J. Proteom. 130 (2016) 85–93.

[35] K. Rajapakse, et al., Proteomic analyses of early response of unicellular eukaryotic microorganism Tetrahymena thermophila exposed to TiO2 particles, Nanotoxicology 10 (2016) 542–556.

[36] M. Planchon, T. Leger, O. Spalla, G. Huber, R. Ferrari, Metabolomic and proteomic investigations of impacts of titanium dioxide nanoparticles on Escherichia coli, PLoS One 12 (2017) e0178437.

[37] D. Hofmann, et al., Mass spectrometry and imaging analysis of nanoparticle-containing vesicles provide a mechanistic insight into cellular trafficking, ACS Nano 8 (2014) 10077–10088.

[38] Y. Tang, et al., Mitochondrial injury induced by nanosized titanium dioxide in A549 cells and rats, Environ. Toxicol. Pharmacol. 36 (2013) 66–72.

[39] E. Huerta-Garcia, S.G. Marquez-Ramirez, G.G. Iglesias, R. Lopez-Marure, Titanium dioxide nanoparticles induce strong oxidative stress and mitochondrial damage in glial cells, Free Radic. Biol. Med. 73 (2014) 84–94.

[40] H. Yin, L. Xu, N.A. Porter, Free radical lipid peroxidation: mechanisms and analysis, Chem. Rev. 111 (2011) 5944–5972.

[41] M. Xiao, H. Zhong, L. Xia, Y. Tao, H. Yin, Pathophysiology of mitochondrial lipid oxidation: role of 4-hydroxynonenal (4-HNE) and other bioactive lipids in mitochondria, Free Radic. Biol. Med. 111 (2017) 316–327.

[42] J.I. Odegaard, A. Chawla, Alternative macrophage activation and metabolism, Annu. Rev. Pathol. 6 (2011) 275–297.
[43] A.M. Scherbart, et al., Contrasting macrophage activation by fine and ultrafine titanium dioxide particles is associated with different uptake mechanisms, Part. Fibre Toxicol. 8 (2011) 31.
[44] A.P. West, G.S. Shadel, S. Ghosh, Mitochondria in innate immune responses, Nat. Rev. Immunol. 11 (2011) 389–402.
[45] F. Grande, P. Tucci, Titanium dioxide nanoparticles: a risk for human health? Mini Rev. Med. Chem. 16 (2016) 762–769.